Passivity Based Power Control of Microgrids ⋆

Juan Carlos Fabián * **Sofía Avila-Becerril** *
Gerardo Espinosa-Pérez *

* *Facultad de Ingeniería, Universidad Nacional Autónoma de México, Ciudad Universitaria, Ciudad de México (e-mail: carlos_jt@hotmail.com; soavbec@comunidad.unam.mx; gerardoe@unam.mx).*

Abstract: In this paper, we recover a passivity based controller previously reported for Microgrids that requires the off–line power flow computation; unlike reported, we propose to generate the desired trajectories dynamically, which allows power control, providing a formal mathematical proof. As a second contribution, we obviate the need to measure active and reactive power by implementing a first order filter. Finally, we present numerical simulations that evaluate our results.

Keywords: Microgrids, Passivity Based Control, Droop Control.

1. INTRODUCTION

Electrical Power Systems (EPS) are changing, to meet the current demands and at the same time to take advantage of all available energy sources, efficient integration of users (as consumers, generators or energy companies) has been sought. Microgrids are part of a new generation of power systems that combine loads, lines, and distributed generation micro–sources (solar panels, small wind turbines, among others) that can be operated in isolation or connected to the main grid(Fang et al. (2012)). Due to the heterogeneous nature of the sources, Microgrids operation is based on power electronics, which gives the compatibility between the energy generated and the demanded by the loads.

For some time now, the study of Microgrids has attracted the attention of the control community (see Barklund et al. (2008); Pedrasa and Spooner (2006); Schiffer et al. (2014), among others). In most of the literature, results lie in an over simplified power converters dynamics accepting the direct application of the so-called droop control, widely used for synchronous generators, which allows controlling the power at the Microgrid nodes.

In this sense, in a previous paper (Avila-Becerril and Espinosa-Pérez (2016)), we show that Hamiltonian properties (see for example Van der Schaft (1999)) of the dynamical model of a Microgrid are preserved even if the dynamic of the power converters are explicitly included. In this case, we reported a tracking controller that stabilizes the Microgrid at the desired voltage value that corresponds to a given steady state power demand. This voltage value is obtained from the off-line solution of the power flow equations, so the drawback is that the controller is not robust against changes in loads. So, a dynamic generation of desired trajectories is needed.

In the same context, and with the aim of evaluating some robustness properties of a PBC scheme, in Avila-Becerril et al. (2017) we incorporate a droop control to generate the desired trajectories and evaluate their performance by means of numerical simulations showing that convergence to the desired behavior is achieved in spite of noise in measurements. The main disadvantage of this result is the lack of a stability proof, the complication comes with the incorporation of the power converters dynamics because on the one hand, the Microgrid model has voltages and currents as states and on the other hand, the droop control needs active and reactive power measurements that, without assuming a steady-state behavior, are not mathematically recoverable, which complicates closing the loop.

The present work extends our results in two directions: Namely, we take the controller presented in Avila-Becerril and Espinosa-Pérez (2016) but propose to dynamically generate the desired state. In this case, we prove that the closed loop trajectories asymptotically tend to a desired and with input-output stability arguments we show that the internal states of the closed loop system are bounded. Second, in order to implement the droop control we propose to recover the active and reactive power by means of the measurement of the instantaneous power, which is only in terms of the product of states model: voltages and currents. Finally, the analysis is evaluated via simulations.

The rest of the paper is organized as follows: For clarity, in Section 2 it is recovered the microgrid structure. Section 3 is devoted to present the controller and the stability proof. In Section 4 we discuss the desired trajectories generation, while in Section 5 the numerical evaluation is carried out. Finally, some concluding remarks are included in Section 6.

⋆ Part of this work was supported by DGAPA-UNAM under grant IN116516.

2. MICROGRID MODEL

In this paper, it is considered a generic balanced microgrid with radial or meshed topology modeled by a single-phase equivalent circuit. Following the proposed in Avila-Becerril and Espinosa-Pérez (2016), we present the subsystems that comprise the model and their port variables, to conclude the section showing the complete microgrid model with PCH structure.

Transmission Lines. Let us begin with the transmission lines and the following assumption:

A.1 Each transmission line is modeled by the π model, *i.e.* a series resistor–inductor (linear) circuit with a capacitor attached to each of its sides.

Assumption **A.1** is typical in power systems literature (see for example Kundur et al. (1994)) for medium transmission lines, and if the line is short the capacitors can be eliminated. Under this assumption, the power network can be represented by an electrical circuit on a graph of n nodes and b edges whose dynamical model is obtained from graph theory. Hence, in order to develop the model, we consider a given tree of the circuit (formed by n nodes and $n-1$ edges so that no loops are formed) with its corresponding co-tree (with the $b-n+1$ edges that do not belong to the tree). Let $i_t, v_t \in \mathbb{R}^{n-1}$ and $i_c, v_c \in \mathbb{R}^{b-(n-1)}$ be the currents and voltages associated to the tree and co-tree respectively; then exploiting the concepts of *basic* cutsets and loopsets of the graph (Wellstead (1979)) the Kirchhoff laws can be expressed as

$$i_t = -Hi_c; \;\; v_c = H^T v_t \tag{1}$$

with the *Fundamental loop matrix* $H \in \mathbb{R}^{(n-1)\times b-(n-1)}$, see Bollobás (1998), which completely characterizes the topology of the circuit.

We also consider, as in Brayton and Moser (1964), that this electrical circuit is *complete* in the sense that all n_1 sources, n_2 capacitors, and n_3 dissipators (the ones in series with the inductances) are tree elements, such that $n = n_1+n_2+n_3$, while all n_3 inductors and the rest of the n_2 dissipators (the loads in parallel with shunt capacitors) are in the co-tree.

Under this partition and Assumption **A.1**, the fundamental loop matrix can be divided as

$$H = \begin{bmatrix} \mathbf{0} & H_{1L} \\ I & H_{CL} \\ \mathbf{0} & I \end{bmatrix}$$

where in each sub-matrix, of appropriate dimensions, $\mathbf{0}$ stands for a matrix full of zeros, I for the identity and the first sub-index stand for tree while the second for co-tree elements (see Avila-Becerril et al. (2016) for details).

For the capacitors and inductors in the circuit, define $x_3 \in \mathbb{R}^{n_2}$ as the electrical capacitor charges vector and $x_4 \in \mathbb{R}^{n_3}$ the linkage inductor fluxes vector, so that the total energy function $H_a : \mathbb{R}^{n_2} \times \mathbb{R}^{n_3} \to \mathbb{R}_{\geq 0}$ is

$$H_a(x_3, x_4) = \frac{1}{2} x_3^T C_a^{-1} x_3 + \frac{1}{2} x_4^T L_a^{-1} x_4 \tag{2}$$

with C_a and L_a the diagonal capacitances and inductances matrices, respectively.

Notice that, under Assumption **A.1**, the dissipators in the tree have the linear constitutive relation

$$i_{Rt} = L_a^{-1} x_4 = R_t^{-1} v_{Rt} \tag{3}$$

where $i_{Rt}, v_{Rt} \in \mathbb{R}^{n_3}$ are the vector currents and voltages on the R-L resistances, $L_a^{-1}x_3$ is inductors current, $R_t = diag\{R_{ti}\} \in \mathbb{R}^{n_3 \times n_3} > 0$ the diagonal resistance matrix, while the current at the i–th load in parallel with the i-th capacitor is

$$i_{Rci} = \psi_{ci}^{-1}(v_{Rci}) = \psi_{ci}^{-1}(C_{ai}^{-1} x_{3i}), \tag{4}$$

with the load voltage v_{Rci} and $\psi_{ci}(\cdot)$ a bijective possibly non-linear function.

Under this conditions, the dynamical model for the network can be written in matrix form as a PCH system,

$$\dot{x}_{34} = (\mathbb{J}_{34} - \mathbb{R}_{34}) P_{34} x_{34} - g_R \Psi_{34} + G_{34} e_1 \tag{5}$$

where $x_{34} = \left[\, x_3^T \;\; x_4^T \,\right]^T \in \mathbb{R}^{(n_1+n_3)}$, $\mathbb{R}_{34} = diag\{0, R_t\}$,

$$\mathbb{J}_{34} = \begin{bmatrix} 0 & -H_{CL} \\ H_{CL}^T & 0 \end{bmatrix} = -\mathbb{J}_{34}^T; \;\; \Psi_{34} = \begin{bmatrix} 0 \\ i_{Rc} \end{bmatrix};$$

$$g_R = \begin{bmatrix} 0 & I \\ I & 0 \end{bmatrix}; \;\; G_{34} = \begin{bmatrix} 0 \\ H_{1L}^T \end{bmatrix}, \;\; P_{34} = \begin{bmatrix} C_a^{-1} & 0 \\ 0 & L_a^{-1} \end{bmatrix}$$

with $i_{Rc}, v_{Rc} \in \mathbb{R}^{n_2}$ the vector of currents and voltages at the loads, subject to the algebraic constraints

$$f_1 = H_{1L} L_a^{-1} x_3 \tag{6}$$

$$v_{Rc} = C_a^{-1} x_3 = \psi_c(i_{Rc}) \tag{7}$$

where $f_1 \in \mathbb{R}^{n_1}$ are the currents vector in the sources. It is important to mention that equation (6) is the current demanded by the transmission lines, but in the sequel, it is assumed ideal sources in the sense that they can provide any amount of current.

Power Converters. We consider n_1 generation units composed by a constant voltage source $V_i \in \mathbb{R} > 0$ modulated by a switching array via $u_i \in \mathbb{R}$ to later on fed a second order LC filter, such that $\mathrm{v}_{Ci} \in \mathbb{R}$ is the output capacitor voltage while $I_{Li} \in \mathbb{R}$ is the port current delivered to the network. The set of n_1 power converters can be represented in port Hamiltonian form with stored energy function $H_c : \mathbb{R}^{n_1} \times \mathbb{R}^{n_1} \to \mathbb{R}_{\geq 0}$ given by

$$H_c(x_1, x_2) = \frac{1}{2} x_1^T L^{-1} x_1 + \frac{1}{2} x_2^T C^{-1} x_2, \tag{8}$$

with the collection of the linkage inductor fluxes $x_1 \in \mathbb{R}^{n_1}$ and $x_2 \in \mathbb{R}^{n_1}$ the electrical capacitor charges, where it has been assumed a linear constitutive relationship for both the inductors and the capacitors, with $L \in \mathbb{R}^{n_1 \times n_1} > 0$ and $C \in \mathbb{R}^{n_1 \times n_1} > 0$ diagonal inductance and capacitance matrices. Define $P_{12} = diag\{L^{-1}, C^{-1}\}$, then the dynamic behavior of the n_1 power converters can be represented by the compact form

$$\dot{x}_{12} = \mathbb{J}_{12} P_{12} x_{12} + G_{12} u - \begin{bmatrix} 0 \\ I_L \end{bmatrix} \tag{9}$$

where $x_{12} = \left[\, x_1^T \;\; x_2^T \,\right]^T \in \mathbb{R}^{n_1}$, the matrices

$$\mathbb{J}_{12} = \begin{bmatrix} 0 & -I \\ I & 0 \end{bmatrix} = -\mathbb{J}_{12}^T \in \mathbb{R}^{n_1 \times n_1}; \;\; G_{12} = \begin{bmatrix} V \\ 0 \end{bmatrix},$$

$u = col(u_i) \in \mathbb{R}^{n_1}$, and the inductor currents vector satisfies $\mathrm{i}_L = L^{-1} x_1 \in \mathbb{R}^{n_1}$, while the capacitor voltages vector is given by $\mathrm{v}_C = C^{-1} x_2 \in \mathbb{R}^{n_1}$.

Remark 1. The structure considered for the power converters essentially captures the dynamic behavior of a large class of these devices since common converter topologies can be represented by a port Hamiltonian structure.

Complete Model. The Hamiltonian model of the microgrid is obtained from (9) and (5) with the following ports selection

$$I_L = H_{1L}\frac{\partial H_a(x_{34})}{\partial x_4} = H_{1L}L_a^{-1}x_4, \quad e_1 = C^{-1}x_2, \quad (10)$$

while the currents at the loads can be written as

$$i_{Rc} = \psi_c^{-1}\left(\frac{\partial H_a(x_{34})}{\partial x_3}\right) = \psi_c^{-1}(x_3) \quad (11)$$

with $\psi_c^{-1}(x_3) = col(\psi_{ci}^{-1}(C_{ai}^{-1}x_{3i}))$. Defining the state $x = \left[\, x_1^T \; x_2^T \; x_3^T \; x_4^T \,\right]^T \in \mathbb{R}^{(3n_1+n_3)}$ and the total stored energy function as

$$H_T(x) = x^T P x, \quad (12)$$

where $P = diag\{L^{-1}, C^{-1}, C_a^{-1}, L_a^{-1}\}$ is the parameters matrix then, the previous models (9), (5), together with (10) and (11), leads to the Microgrids complete model

$$\dot{x} = (\mathbb{J}_T - \mathbb{R}_T)Px - g_{RT}\Psi_{34}(x_3) + G_T u \quad (13)$$

with $\mathbb{R}_T = diag\{0, 0, 0, R_t\} \geq 0$ and the matrices of appropriate dimensions

$$\mathbb{J}_T = \begin{bmatrix} 0 & -I & 0 & 0 \\ I & 0 & 0 & -H_{1L} \\ 0 & 0 & 0 & -H_{CL} \\ 0 & H_{1L}^T & H_{CL}^T & 0 \end{bmatrix} = -\mathbb{J}_T^T; \quad g_{RT} = \begin{bmatrix} 0 & 0 \\ 0 & 0 \\ 0 & I \\ 0 & 0 \end{bmatrix};$$

$$G_T u = \begin{bmatrix} Vu \\ 0 \\ 0 \\ 0 \end{bmatrix} \quad \Psi_{34}(x_3) = \begin{bmatrix} 0 \\ \psi_c^{-1}(x_3) \end{bmatrix}.$$

Likewise, the *admissible trajectories* are the solutions of

$$\dot{x}^\star = (\mathbb{J}_T - \mathbb{R}_T)Px^\star - g_{RT}\Psi_{34}^\star(x_3^\star) + G_T u^\star, \quad (14)$$

with $u^\star$ the control input that generates $x^\star$. With the definition of the desired system, the error variable is set as $\tilde{x} = x - x^\star$ and their corresponding error dynamic is

$$\dot{\tilde{x}} = (\mathbb{J}_T - \mathbb{R}_T)P\tilde{x} - g_{RT}\left[\Psi_{34}(x_3) - \Psi_{34}^\star(x_3^\star)\right] + G_T\tilde{u}$$

where $\tilde{u} = u - u^\star$ and the associated energy–like function

$$\tilde{H}_T(\tilde{x}) = \frac{1}{2}\tilde{x}^T P\tilde{x}. \quad (15)$$

Now, it is possible to formulate the main stabilization result of the paper.

3. MAIN RESULT: MICROGRID STABILIZATION

In this section, we recover the controller for each converter proposed in Avila-Becerril and Espinosa-Pérez (2016) and we prove that the system achieves asymptotically a given dynamic desired inverter voltage $C^{-1}x_2^\star$, with internal stability, leaving to Section 4 a discussion on the selection of the reference that takes into account the power demand, by means of a droop–like control.

Proposition 1. Consider a Microgrid system of the form (13) and assume

A.2 The state x_{12} and the output current f_1 are available for measurement.
A.3 The P parameters matrix is known.
A.4 The prescribed steady–state behavior $x_2^\star$ is a known continuous function, bounded and with bounded second derivative.
A.5 The load port–variables satisfies the passivity requirement

$$(v_{Rc} - v_{Rc}^\star)^T\left[\psi_c^{-1}(v_{Rc}) - \psi_c^{-1}(v_{Rc}^\star)\right] > 0 \quad (16)$$

Under these conditions, the control law

$$u = V^{-1}[\dot{x}_1^\star + C^{-1}x_2^\star - K_1 L^{-1}\tilde{x}_1] \quad (17)$$

with the desired state satisfying the constraints

$$\dot{x}_2^\star - L^{-1}x_1^\star + H_{1L}L_a^{-1}x_4^\star - K_2 C^{-1}\tilde{x}_2 = 0, \quad (18a)$$

$$\dot{x}_3^\star + H_{CL}L_a^{-1}x_4^\star + \psi_c^{-1}(C_a^{-1}x_3^\star) = 0 \quad (18b)$$

$$\dot{x}_4^\star - H_{1L}^T C^{-1}x_2^\star - H_{CL}^T C_a^{-1}x_3^\star + R_t L_a^{-1}x_4^\star = 0 \quad (18c)$$

with the positive diagonal gain matrices $K_1, K_2 \in \mathbb{R}^{n_1\times n_1}$ guarantees that

$$lim_{t\to\infty}\tilde{x} = 0$$

guaranteeing internal stability.

Proof. The control law in equations (17) and (18) can be equivalently written as

$$G_T\tilde{u} = -\mathbb{K}_T P\tilde{x}$$

with $\mathbb{K}_T = diag\{K_1, K_2, 0, 0\} \in \mathbb{R}^{(3n_1+n_3)\times(3n_1+n_3)} > 0$. Using this expression, the closed loop system takes the form

$$\dot{\tilde{x}} = [\mathbb{J}_T - \mathbb{R}_T - \mathbb{K}_T]P\tilde{x} - g_{RT}\begin{bmatrix} 0 \\ \psi_c^{-1}(x_3) - \psi_c^{-1}(x_3^\star) \end{bmatrix}. \quad (19)$$

To analyze the origin of the closed-loop system we consider (15) as a Lyapunov function, its time derivative along the trajectories of (19) is given by

$$\begin{aligned}\dot{\tilde{H}}_T(\tilde{x}) = &- \tilde{x}^T P(\mathbb{R}_T + \mathbb{K}_T)P\tilde{x} \\ &- C_a^{-1}\tilde{x}_3\left[\psi_c^{-1}(x_3) - \psi_c^{-1}(x_3^\star)\right].\end{aligned}$$

Furthermore, since the characteristic function $\psi_c^{-1}(\cdot)$ satisfy condition (16), with the voltages $v_{Rc} = C_a^{-1}x_3$, on Proposition 1 then

$$\dot{\tilde{H}}_T \leq -\tilde{x}^T P(\mathbb{R}_T + \mathbb{K}_T)P\tilde{x} \leq 0, \quad (20)$$

and therefore the function $\tilde{H}_T$ is non-increasing and its argument $\tilde{x}$ is bounded. Moreover, $\dot{\tilde{H}}$ is zero only at the origin $\tilde{x} = 0$ which ensures asymptotic stability of the equilibrium point.

Even though it has been proven that the error tends to zero, the trajectories could tend to infinity for desired unbounded trajectories. For this, it is important to note that in Proposition 1 it is only necessary to know *a priori* the voltage $C_a^{-1}x_2^\star$. In the following, it will be shown that if $C_a^{-1}x_2^\star$ is bounded, then all the desired state is also bounded.

From (20) and Proposition 1 we know that $\tilde{x}_1, \tilde{x}_2, x_2^\star, \dot{x}_2^\star$ and $\ddot{x}_2^\star$ are bounded signals; so in order to guarantee that the control law $u = f(\tilde{x}_1, \dot{x}_1^\star, x_2^\star) \in L_\infty$, it must be ensured that $\dot{x}_1^\star$ is also L_∞. Now, let us rewrite equations (18a–18c) as

$$x_1^\star = L\left(\dot{x}_2^\star + H_{1L}L_a^{-1}x_4^\star - K_2C^{-1}\tilde{x}_2\right) \tag{21a}$$

$$\begin{bmatrix}\dot{x_3}^\star \\ \dot{x_4}^\star\end{bmatrix} = \begin{bmatrix}0 & -H_{CL} \\ H_{CL}^T & -R_t\end{bmatrix}\begin{bmatrix}C_a^{-1}x_3^\star \\ L_a^{-1}x_4^\star\end{bmatrix} + \begin{bmatrix}-\psi_c^{-1}(x_3^\star) \\ H_{1L}^TC^{-1}x_2^\star\end{bmatrix} \tag{21b}$$

It can be noticed that $x_1^\star$ is an algebraic function of $(\dot{x}_2^\star, \tilde{x}_2, x_4^\star)$ with the first two signals bounded. So the rationale is that if $x_4^\star$ is L_∞, then $x_1^\star, \dot{x}_1^\star \in L_\infty$ and consequently $u \in L_\infty$. So it is necessary to analyze the subsystem $\dot{x}_{34}^\star$ in (21b) which has $x_2^\star$ as input.

With the aim of showing that $x_{34}^\star$ is bounded, take the positive function $H_{34}^\star : \mathbb{R}^{n_2+n_3} \to \mathbb{R}$ given by

$$H_{34}^\star(x_{34}^\star) = \frac{1}{2}(x_{34}^\star)^T P_{34} x_{34}^\star. \tag{22}$$

The time derivative of (22) along (21b) is

$$\begin{aligned}\dot{H}_{34}^\star &= (x_{34}^\star)^T P_{34}\left((\mathbb{J}_{34} - \mathbb{R}_{34})P_{34}x_{34}^\star + \begin{bmatrix}-\psi_c^{-1}(x_3^\star) \\ H_{1L}^TC^{-1}x_2^\star\end{bmatrix}\right) \\ &= -(x_{34}^\star)^T P_{34}\mathbb{R}_{34}P_{34}x_{34}^\star + (x_{34}^\star)^T P_{34}\begin{bmatrix}-\psi_c^{-1}(x_3^\star) \\ H_{1L}^TC^{-1}x_2^\star\end{bmatrix} \\ &= -(L_a^{-1}x_4^\star)^T R_t L_a^{-1}x_4^\star - (C_a^{-1}x_3^\star)^T\psi_c^{-1}(x_3^\star) + \\ &+ (L_a^{-1}x_4^\star)^T C^{-1}x_2^\star. \end{aligned} \tag{23}$$

Note that, for passive loads, the second term on the right side $(C_a^{-1}x_3^\star)^T\psi_c^{-1}(x_3^\star) > 0$, that is the product of voltage times current.

From $\dot{H}_{34}^\star$ it is clear that the unforced system

$$\dot{x}_{34}^\star = f(x_{34}^\star, 0)$$

has an asymptotically stable equilibrium point at the origin $x_{34}^\star = 0$. Define $z_4 := L_a^{-1}x_4^\star$ and $z_2 := C^{-1}x_2^\star$ then, equation (23) can also be written as

$$\begin{aligned}\dot{H}_{34}^\star &= -(1-\theta)(z_4^TR_tz_4) - \theta(z_4^TR_tz_4) \\ &\quad - (C_a^{-1}x_3^\star)^T\psi_c^{-1}(x_3^\star) + z_4^Tz_2 \\ \dot{H}_{34}^\star &\leq -(1-\theta)(z_4^TR_tz_4), \quad \forall\, |z_4| \geq \left(\frac{|z_2|}{\theta\lambda_{min}\{R_t\}}\right)\end{aligned}$$

where $0 < \theta < 1$. Thus, the system is input to state–stable, which means that for any bounded $x_2^\star$, the state $x_4^\star$, and $x_3^\star$, will be bounded, which completes the proof. ■

Evidently, now the problem lies in the selection of the desired voltage $C^{-1}x_2^\star$, so in the next section we discuss this question.

4. STEADY–STATE BEHAVIOR

In a general context, the desired is stated in terms of the power demanded by the loads. Once the power demand is fixed, the converters must be able to supply it. We assume that in steady–state each power converter has a voltage

$$C_i^{-1}x_{2i}^\star = V_{2i}^\star \sin(\omega_s t + \delta_i^\star), \tag{24}$$

where $\omega_s \in \mathbb{R}$ takes the same value for all the power converters, while the magnitude $V_{2i}^\star$ and the phase δ_i must be determined. Let the complex admittance be denoted as $Y_{ik} := G_{ik} + jB_{ik} \in \mathbb{C}$ with conductance G_{ik} and susceptance B_{ik} and let $\mathcal{N}_i$ be the set of neighbors of the $i-th$ node for which $Y_{ik} \neq 0$. That said, the desired active and reactive power (see Kundur et al. (1994)) at the $i-th$ node $P_i^\star$ and $Q_i^\star$ are obtained as

$$\begin{aligned}P_i^\star &= G_{ii}V_i^2 - \sum_{k\sim\mathcal{N}_i} V_iV_k(G_{ik}\cos\delta_{ik} + B_{ik}\sin\delta_{ik}) \\ Q_i^\star &= -B_{ii}V_i^2 - \sum_{k\sim\mathcal{N}_i} V_iV_k(G_{ik}\sin\delta_{ik} - B_{ik}\cos\delta_{ik})\end{aligned} \tag{25}$$

where

$$G_{ii} \triangleq \hat{G}_{ii} + \sum_{k\sim\mathcal{N}_i} G_{ik}, \text{ and } B_{ii} \triangleq \hat{B}_{ii} + \sum_{k\sim\mathcal{N}_i} B_{ik},$$

with $\hat{G}_{ii} \in \mathbb{R}$ and $\hat{B}_{ii} \in \mathbb{R}$ the shunt conductance and susceptance, while $\delta_{ik} \triangleq \delta_i - \delta_k$.

Thus, we propose to fix the active and reactive power at the loads, at a constant nominal operation, and solve (offline) equations (25) in order to calculate the desired magnitude $V_{2i}^\star$ and the phases $\delta_i^\star$ of the n_1 converter nodes. Once founded the voltages $C_i^{-1}x_{2i}^\star = A_i^\star\sin(\omega_s t + \delta_i^\star)$ that meets the load power demand, equation (21b) can be solve for $x_4^\star$ and then the restriction (18a) is incorporated for $x_1^\star \in \mathbb{R}^{n_1}$ such that the control law $u \in \mathbb{R}^{n_1}$ in (17) can be implemented.

A drawback of the proposed solution lies in the necessity to compute off-line the admissible trajectories $C^{-1}x_2^\star$; so, with the aim of including a dynamic mechanism to compute these values taking into account the power demand, in the following subsection we incorporate a droop–like control.

4.1 Droop control

The droop control is widely used for synchronous generators (Kundur et al. (1994)) where a change in the active power demand is reflected as a change in the system's frequency, which in turn modify electrical torque, generating speed variations. Basically, the droop control is a proportional control that allows the specification of the steady state power and is usually (see Schiffer et al. (2014), Simpson-Porco et al. (2013) and references therein) implemented as

$$\begin{aligned}u_{i1} &= \omega_d - k_{pi}\left(P_i - P_{id}\right), \\ u_{i2} &= V_{id} - k_{qi}\left(Q_i - Q_{id}\right),\end{aligned} \tag{26}$$

with ω_d, V_{id}, P_{id} y Q_{id} reference points delivered by an external controller, k_{pi} and k_{qi} the control gains, and P_i, Q_i the active and reactive measures powers. Intending to reap the benefits of droop control, in Avila-Becerril et al. (2017) it was proposed to set the desired voltages of the power converters $C^{-1}x_2^\star$ as

$$C_i^{-1}x_{2i}^\star = V_i^\star \sin(\dot{\delta}_i^\star t), \tag{27}$$

$$\begin{aligned}V_i^\star &= V_{ird} - k_{qi}\left(Q_i - Q_{id}\right), \\ \dot{\delta}_i^\star &= \omega_{rd} - k_{pi}\left(P_i - P_{id}\right),\end{aligned} \tag{28}$$

with V_{ird} and ω_{rd} the desired voltages and frequencies. It can be noticed that the right-hand side of equation (27) corresponds to (26), so it has used the droop control to propose the magnitude and frequency of the desired trajectories for the controller.

For implementation purposes, it is now necessary to measure the active and reactive power at the nodes with converters. However, it is important to mention that, under these new conditions, the stability proof presented above is no longer true, since the generation of the desired trajectories now implicitly depends on the states of the system. In particular, P_i and Q_i in (25) are non-linear functions of the voltage *magnitude* and *phase* of the voltage $C_i^{-1}x_{2i}$. So, in order to recognize the structure of the closed loop system, and inspired in Furtado et al. (2008), we propose to recover the active and reactive power from the instantaneous power, which is in terms of the states.

Define the instantaneous power as the product of current by voltage as

$$p_{ins}(t) = v(t)i(t) \tag{29}$$

In the case of the converters, the instantaneous power will be $p_{ins}(t) = H_{1L}L_a^{-1}x_4C^{-1}x_2$, and if we are interested in the loads, then $p_{ins}(t) = C_a^{-1}x_3\psi_c^{-1}(x_3)$. One way to recover the active power, based on the fact that the average reactive power is zero, is by low-pass filtering the instantaneous power

$$\dot{P} = \omega_f\left(-P + p_{ins}\right) \tag{30}$$

where ω_f is the associated low-pass filter cutoff angular frequency, while the reactive power can be directly obtained from the instantaneous power as

$$Q = p_{ins} - P \tag{31}$$

With equations (29) and (30–31) at hand, it is possible to close the control loop and thereby to find a structure for the system. Current efforts are developed on this issue.

5. NUMERICAL EVALUATION

In order to evaluate the controller proposed above we present some numerical results for two scenarios: First, we introduce the solution for the power flow equations and use it to give the reference values (24) needed for the controller implementation; and second, we use the droop control in equation (28) to generate the reference (27). In the two cases, we use a five nodes meshed network, shown in Figure 1 and taken from Stagg and El-Abiad (1968), which has two nodes with inverters connected with three loads–nodes through power lines with parameters depicted in Table 1. In the case of the power converters,

Table 1. Impedances and line charging

Bus	Impedance	Line charging
1-2	0.02+j0.06	0.0+j0.030
1-3	0.08+j0.24	0.0+j0.025
2-3	0.06+j0.18	0.0+j0.020
2-4	0.06+j0.18	0.0+j0.020
2-5	0.04+j0.12	0.0+j0.015
3-4	0.01+j0.03	0.0+j0.010
4-5	0.08+j0.24	0.0+j0.025

we set their filter parameters as $C_i = 1.2\times10^{-4}$[F], $L_i = 5.8635\times10^{-4}$[H], and $V_i = 1.3pu$. In addition, the control gains have been fixed in $\mathbb{K}_T = diag\{3I_2, 3I_2, 0, 0\}$, with I_2 the identity, for both cases. The numerical evaluation was performed in MATLAB2016a with fixed step, ode4 Runge-Kutta integration method and all initial condition were set to zero.

In the first scenario, we fixed the active and reactive power at the loads and we have used the power flow analysis to calculate the magnitude and phase voltages needed at the nodes 1 and 2. The values obtained, from Gauss Seidel method, are shown in Table 2, with the base

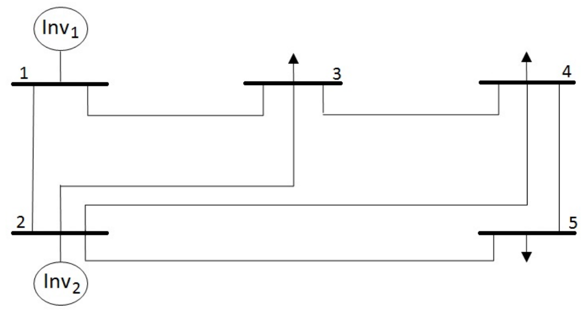

Fig. 1. Power network

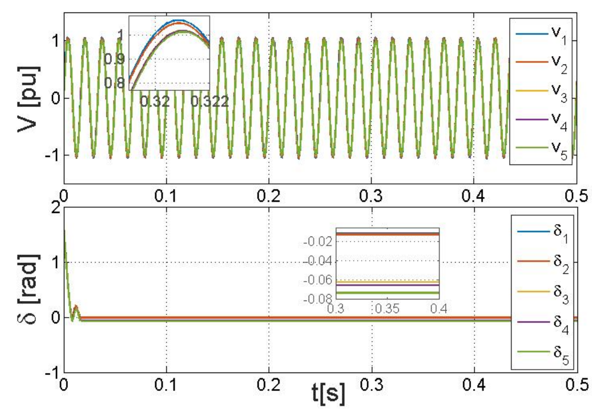

Fig. 2. First Case: Voltage and phase angle

units in the calculations per unit $S_B = 100MVA$, $V_B = 100KV$ and $Z_{base} = 100[\Omega]$. Figure 2, present the bounded voltage signal and the phase of each node that coincide with the values in Table 2; specifically, Figure 3 shows that the tracking control problem is solved and that with a bounded input the state is also bounded, which supports the stated in this paper. Finally, notice that the power demand is satisfied, this is showed in Figure 4.

Table 2. Data from power flow

	Bus voltages
Bus 2	1.0476 ∠-0.0489
Bus 3	1.0244∠-0.0872
Bus 4	1.0237∠-0.0930
Bus 5	1.0181∠-0.1073

For the second scenario, the droop gains were fixed in $k_{p1} = k_{p2} = 0.012$, ,$k_{q1} = k_{q2} = 0.006$, and $\omega_{f1} = 40$, $\omega_{f2} = 7$ for the low-pass filters cutoff frequencies in equation (30). Similar to the first case, Figure 5 presents the tracking error, to exhibit the performance of the controller under the feedback of the instantaneous power via equations (30) and (31), while Figure 6 presents the active and reactive power measured in the five nodes that coincide with the ones in Figure 4, which allows concluding that the controller is robust under a time varying reference calculation and that filter (30) is a good approach to the measured active and reactive power.

6. CONCLUSION

In this paper, we recovered a controller that solves a tracking voltage problem for Microgrids, which, unlike as

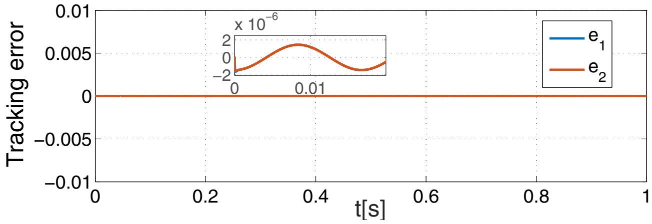

Fig. 3. First Case: Tracking error $\tilde{x}_2$

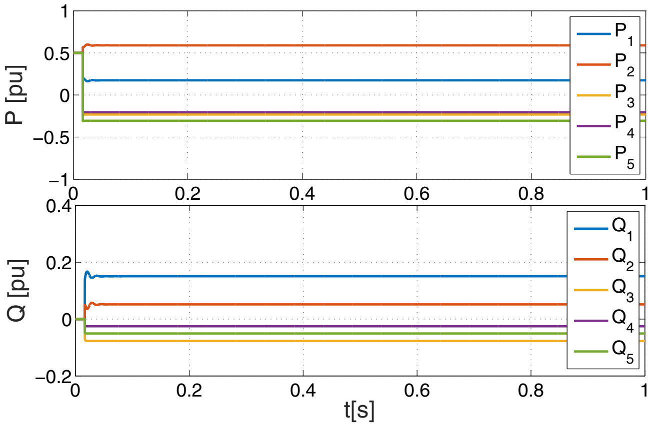

Fig. 4. First Case: Active and reactive power

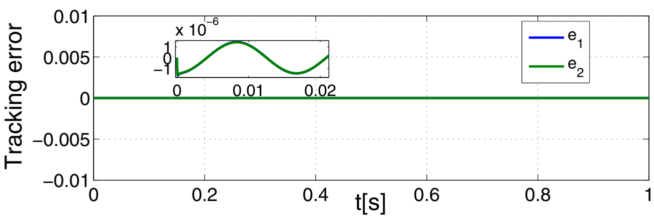

Fig. 5. Second Case: Tracking error $\tilde{x}_2$

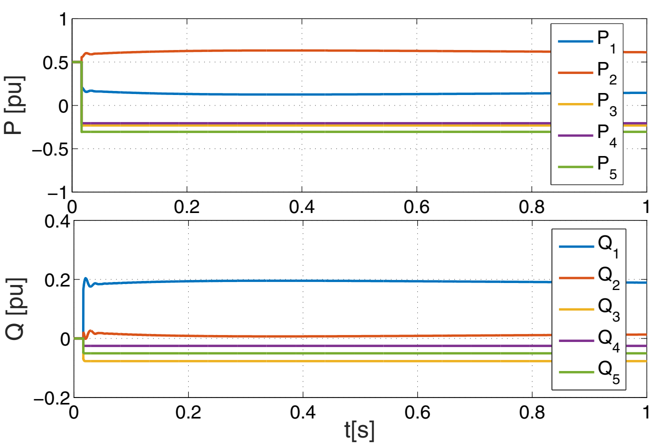

Fig. 6. Second Case: Active and reactive power

is usual in the literature, includes the power converters dynamics. In this sense, we have extended our previous result by dynamically generate the converters voltage reference with the power demand information. In this case, we also have avoided the measurement of active and reactive power by means of a first order filter with instantaneous power measurement as input; this is attractive for analysis purposes because now the measurements are in terms of the state. Although still working on the stability proof of this controller, the numerical simulations show a proper performance.

REFERENCES

Avila-Becerril, S. and Espinosa-Pérez (2016). A hamiltonian approach for stabilization of microgrids including power converters dynamic. *Congreso Latinoamericano de Control Automático CLCA, 2016*, 246–251.

Avila-Becerril, S., Silva-Martínez, D., and Espinosa-Pérez, G. (2017). On the robustness of a passivity-based controller for microgrids. *World Congress of the International Federation of Automatic Control, IFAC, 2017 (accepted)*.

Avila-Becerril, S., Espinosa-Pérez, G., and Fernandez, P. (2016). Dynamic characterization of typical electrical circuits via structural properties. *Mathematical Problems in Engineering*, 2016.

Barklund, E., Pogaku, N., Prodanović, M., Hernandez-Aramburo, C., and Green, T.C. (2008). Energy management in autonomous microgrid using stability-constrained droop control of inverters. *Transactions on Power Electronics, IEEE*, 23(5), 2346–2352.

Bollobás, B. (1998). *Modern graph theory*, volume 184. Springer Science & Business Media.

Brayton, R. and Moser, J. (1964). A theory of nonlinear networks i. *Quart. Appl. Math*, 22(1), 1–33.

Fang, X., Misra, S., Xue, G., and Yang, D. (2012). Smart grid—the new and improved power grid: A survey. *Communications Surveys & Tutorials, IEEE*, 14(4), 944–980.

Furtado, E.C., Aguirre, L.A., and Tôrres, L.A. (2008). Ups parallel balanced operation without explicit estimation of reactive power—a simpler scheme. *IEEE Transactions on Circuits and Systems II: Express Briefs*, 55(10), 1061–1065.

Kundur, P., Balu, N., and Lauby, M. (1994). *Power system stability and control*, volume 7. McGraw-hill New York.

Pedrasa, M.A. and Spooner, T. (2006). A survey of techniques used to control microgrid generation and storage during island operation. In *Proceedings of the 2006 Australasian Universities Power Engineering Conference (AUPEC'06)*, 1–6.

Schiffer, J., Ortega, R., Astolfi, A., Raisch, J., and Sezi, T. (2014). Conditions for stability of droop-controlled inverter-based microgrids. *Automatica*, 50(10), 2457–2469.

Simpson-Porco, J.W., Dörfler, F., and Bullo, F. (2013). Synchronization and power sharing for droop-controlled inverters in islanded microgrids. *Automatica*, 49(9), 2603–2611.

Stagg, G.W. and El-Abiad, A.H. (1968). *Computer methods in power system analysis*. McGraw-Hill.

Van der Schaft, A. (1999). *L2-gain and passivity in nonlinear control*. Springer-Verlag New York, Inc.

Wellstead, P. (1979). *Introduction to physical system modelling*. Academic Press London.